PERGAMON

International Journal of Solids and Structures 36 (1999) 3375–3390

INTERNATIONAL JOURNAL OF SOLIDS and STRUCTURES

Multiple parallel cracks interaction problem in piezoelectric ceramics

Jian-Jun Han*, Yi-Heng Chen

School of Civil Engineering and Mechanics, Xi'an Jiaotong University, 710049, P.R. China

Received 16 January 1998; in revised form 9 April 1998

Abstract

This paper has two goals. First, we propose the 'pseudo-traction–electric displacement' method for solving the interaction problem of multiple parallel cracks in transversely isotropic piezoelectric ceramics. Second, we present a fundamental understanding for the role that the electric displacement loading plays in the interaction problem. Detailed comparisons between the results under the compound mechanical–electric loading conditions and those derived under purely mechanical loading conditions are performed. It is shown that the mechanical fracture parameters such as the stress intensity factors are no longer independent of the electric loading as they would be in single crack problems. Quite contrary, the electric displacement loading has a significant influence on the stress intensity factors, the total potential energy release rate and the mechanical strain energy release rate. This important conclusion is mainly due to the interaction effect, i.e., one of the multiple cracks releases the stresses and disturbs the electric fields near the other crack. It is also found that there are some special relative locations for the multiple parallel cracks at which the electric displacement loading has no effect on the Mode I stress intensity factor. However, the mechanical strain energy release rate has no such a property.

1. Introduction

Fracture problems in piezoelectric media have received considerable attention in the past ten years. Sosa and Pak (1990), Sosa (1991, 1992), Pak (1990, 1992) and Suo et al. (1992) investigated the crack problems in two-dimensional piezoelectric ceramics. The fracture parameters: the stress intensity factors (SIF's), the electric displacement intensity factor (EDIF) and the potential energy release rate (TPERR or the *J*-integral) are defined by them. This made a good foundation of fracture mechanics of piezoelectric ceramics. Recently, Pak and Sun (1995a, b) have shown that the SIF's and the TPERR are not suitable for describing the fracture behavior of piezoelectric ceramics. Thus, they proposed a new fracture criterion based on the mechanical strain energy

* Corresponding author. E-mail: wsry@sun20.xjtu.edu.cn

0020–7683/99/$ - see front matter
PII: S0020–7683(98)00149–8

release rate (MSERR). The conclusions derived by them agree with experimental evidences which show that the positive electric fields aid the crack propagation, while the negative electric fields impede crack propagation. Pak and Carman (1997) have shown that electric fatigue of piezoceramics is attributable to the presence of internal defects. Moreover, they present an analytical solution to calculate the stress concentrations around an elliptical void under purely electric loading. Under the condition of neglecting the interaction effect among the defects, they concluded that there exists an optimal property of the piezoelectric ceramics for eliminating the stress concentrations. What is more, this optimal property is independent of the defect geometry such that it could be applied to the crack problems.

In this study, the authors address their attention on the interaction problem of multiple parallel cracks in transversely isotropic piezoelectric ceramics. First, the elementary solution of a finite crack subjected to concentrated forces and concentrated electric displacements on the crack faces is derived in Section 2. After doing so, the 'pseudo-traction–electric displacement' (PTED) method is proposed and a system of integral equations is deduced in Section 3. Finally, several numerical examples are presented and the results of the interaction problems under the compound mechanical–electric loading conditions are compared in Section 4 with those derived previously under purely mechanical loading conditions. Since one of the multiple cracks releases the stresses and disturbs the electric fields induced by the electric loading near the other crack, the mechanical parameters such as SIF's are no longer independent of the electric loading as they would be in single crack problems shown by Sosa (1992) and Pak (1992). Quite contrary, the results show that the electric displacement effect plays an important role in the present interaction problems of multiple cracks. From the results obtained in this paper, it can also be seen that the electric displacement loading may have increasing or decreasing effects on the Mode I SIF. Moreover, these effects are governed by the electric displacement loading level and the relative location of the multiple cracks. The positive electric displacement loading has increasing effects for some location angles, while it has decreasing effects for other location angles. On the contrary, the negative electric displacement loading has converse effects from the effects of positive electric displacement loading for the same location angles. The location distance mainly influences the intensity of the interaction effect. Thus, the larger location distance makes the interaction effect weaker, while the small location distance makes it stronger. It can also be seen that the electric displacement loading has more significant influence on the mechanical strain energy release rate (MSERR) than that on the Mode I SIF and the positive electric displacement loading makes the MSERR increase, while the negative electric displacement loading leads to the MSERR decreasing. Furthermore, the MSERR changes linearly as the electric displacement loading increases in the interaction problems, although the slope is changed comparing with the slope in single crack problems. However, in the collinear cases of multiple cracks, the mechanical loading and the electric loading are uncoupled. Therefore, the mechanical loading only influences the SIF's, while the electric loading only affects the EDIF in these special circumstances.

2. Elementary solutions

Consider the two-dimensional problem in transversely isotropic piezoelectric ceramics under plane strain conditions. The y-axis shown in Fig. 1 is parallel to the poling direction of the piezoelectric materials. Then, the constitutive equations can be written as (Sosa, 1992):

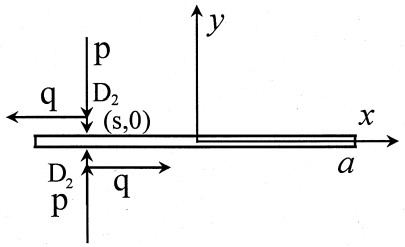

Fig. 1. A finite crack is subjected to concentrated loading.

$$\begin{Bmatrix}\varepsilon_{11}\\ \varepsilon_{22}\\ 2\varepsilon_{12}\end{Bmatrix}=\begin{bmatrix}a_{11} & a_{12} & 0\\ a_{12} & a_{22} & 0\\ 0 & 0 & a_{33}\end{bmatrix}\begin{Bmatrix}\sigma_{11}\\ \sigma_{22}\\ \sigma_{12}\end{Bmatrix}+\begin{bmatrix}0 & b_{21}\\ 0 & b_{22}\\ b_{13} & 0\end{bmatrix}\begin{Bmatrix}D_1\\ D_2\end{Bmatrix}$$

$$\begin{Bmatrix}E_1\\ E_2\end{Bmatrix}=-\begin{bmatrix}0 & 0 & b_{13}\\ b_{21} & b_{22} & 0\end{bmatrix}\begin{Bmatrix}\sigma_{11}\\ \sigma_{22}\\ \sigma_{12}\end{Bmatrix}+\begin{bmatrix}\delta_{11} & 0\\ 0 & \delta_{22}\end{bmatrix}\begin{Bmatrix}D_1\\ D_2\end{Bmatrix} \tag{1}$$

where, ε_{ij}, σ_{ij}, D_i and E_i are strain, stress, electric displacement and electric field, respectively and a_{ij}, b_{ij} and δ_{ii}, are reduced material constants.

The stress and the electric displacement components can be expressed by three complex potentials $\Phi_k(Z_k)$ $(k=1,2,3)$ from the following relations (Sosa, 1992):

$$\sigma_{11}=G_4(\Phi_k(Z_k),Z_k)=\sum_{k=1}^{3}[\mu_k^2\Phi_k(Z_k)+\overline{\mu_k^2\Phi_k(Z_k)}]$$

$$\sigma_{22}=G_1(\Phi_k(Z_k),Z_k)=\sum_{k=1}^{3}[\Phi_k(Z_k)+\overline{\Phi_k(Z_k)}]$$

$$\sigma_{12}=G_2(\Phi_k(Z_k),Z_k)=-\sum_{k=1}^{3}[\mu_k\Phi_k(Z_k)+\overline{\mu_k\Phi_k(Z_k)}]$$

$$D_1=G_5(\Phi_k(Z_k),Z_k)=\sum_{k=1}^{3}[\lambda_k\mu_k\Phi_k(Z_k)+\overline{\lambda_k\mu_k\Phi_k(Z_k)}]$$

$$D_2=G_3(\Phi_k(Z_k),Z_k)=-\sum_{k=1}^{3}[\lambda_k\Phi_k(Z_k)+\overline{\lambda_k\Phi_k(Z_k)}] \tag{2}$$

where the overbar denotes the complex conjugation and:

$$Z_k=x+\mu_k y$$

$$\lambda_k=[(b_{21}+b_{13})\mu_k^2+b_{22}]/(\delta_{11}\mu_k^2+\delta_{22})\quad(k=1,2,3) \tag{3}$$

μ_k are three roots with positive imaginary parts of the following governing equation:

$$A\mu^6 + B\mu^4 + C\mu^2 + D = 0 \tag{4}$$

where

$$\begin{aligned} A &= a_{11}\delta_{11} \\ B &= a_{11}\delta_{22} + 2a_{12}\delta_{11} + a_{33}\delta_{11} + b_{21}^2 + b_{13}^2 + 2b_{21}b_{13} \\ C &= a_{22}\delta_{11} + 2a_{12}\delta_{22} + a_{33}\delta_{22} + 2b_{21}b_{22} + 2b_{13}b_{22} \\ D &= a_{11}\delta_{11} + b_{22}^2 \end{aligned} \tag{5}$$

As shown in Fig. 1, a finite crack with length $2a$ in an infinite piezoelectric ceramic is loaded by the concentrated forces P and q and the concentrated electric displacement D_2 on the crack faces. The poling direction of the material is assumed to be the direction of the y-axis.

From the conditions:

$$\begin{aligned} &\sigma_{22}^{+}(x) = \sigma_{22}^{-}(x) \\ &\sigma_{12}^{+}(x) = \sigma_{12}^{-}(x) \quad (y = 0) \\ &D_2^{+}(x) = D_2^{-}(x) \end{aligned} \tag{6}$$

we can obtain the following relations:

$$\begin{aligned} &\sum_{k=1}^{3} [\Phi_k(x) - \bar{\Phi}_k(x)]^{+} = \sum_{k=1}^{3} [\Phi_k(x) - \bar{\Phi}_k(x)]^{-} \\ &\sum_{k=1}^{3} [\mu_k\Phi_k(x) - \overline{\mu_k}\bar{\Phi}_k(x)]^{+} = \sum_{k=1}^{3} [\mu_k\Phi_k(x) - \overline{\mu_k}\bar{\Phi}_k(x)]^{-} \\ &\sum_{k=1}^{3} [\lambda_k\Phi_k(x) - \overline{\lambda_k}\bar{\Phi}_k(x)]^{+} = \sum_{k=1}^{3} [\lambda_k\Phi_k(x) - \overline{\lambda_k}\bar{\Phi}_k(x)]^{-} \end{aligned} \tag{7}$$

which are the well-known simplest Rieman–Hilbert problems, whose solutions are complex holomorphic functions. According to the remote conditions, the functions should be zero in the present problem without doubt. Then, the following relations are derived:

$$\begin{aligned} &\sum_{k=1}^{3} \Phi_k(Z_k) = \sum_{k=1}^{3} \bar{\Phi}_k(Z_k) \\ &\sum_{k=1}^{3} \mu_k\Phi_k(Z_k) = \sum_{k=1}^{3} \overline{\mu_k}\bar{\Phi}_k(Z_k) \\ &\sum_{k=1}^{3} \lambda_k\Phi_k(Z_k) = \sum_{k=1}^{3} \overline{\lambda_k}\bar{\Phi}_k(Z_k) \end{aligned} \tag{8}$$

The boundary conditions on the crack faces as shown in Fig. 1 are:

$$\sigma_{22}^{+}(x) = \sigma_{22}^{-}(x) = P\delta(x - s)$$

$$\sigma_{12}^{+}(x=\sigma_{12}^{-}(x)=Q\delta(x-s) \quad (y=0,|x|<a)$$

$$D_2^{+}(x)=D_2^{-}(x)=D_2\delta(x-s) \tag{9}$$

Substituting eqns (2) into eqns (9), the following relations are obtained:

$$\sum_{k=1}^{3}[\Phi_k^{+}(x)+\bar{\Phi}_k^{-}(x)]=P\delta(x-s)$$

$$\sum_{k=1}^{3}[\mu_k\Phi_k^{+}(x)\overline{\mu_k}\bar{\Phi}_k^{-}(x)]=-Q\delta(x-s)$$

$$\sum_{k=1}^{3}[\lambda_k\Phi_k^{+}(x)+\overline{\lambda_k}\bar{\Phi}_k^{-}(x)]=-D_2\delta(x-s) \tag{10}$$

After substituting eqn (8) into eqn (10), a system of linear equations is derived whose solutions are:

$$\Phi_k^{+}(x)+\Phi_k^{-}(x)=(A_{k1}P+A_{k2}Q+A_{k3}D_2)\delta(x-s) \quad (k=1,2,3) \tag{11}$$

where A_{ij} are complex elements of the following complex matrix:

$$A=[A_{ij}]=\frac{1}{\Delta}\begin{bmatrix}\mu_2\lambda_3-\mu_3\lambda_2 & \lambda_3-\lambda_2 & \mu_2-\mu_3\\ \mu_3\lambda_1-\mu_1\lambda_3 & \lambda_1-\lambda_3 & \mu_3-\mu_1\\ \mu_1\lambda_2-\mu_2\lambda_1 & \lambda_2-\lambda_1 & \mu_1-\mu_2\end{bmatrix} \tag{12}$$

where

$$\Delta=\mu_1(\lambda_2-\lambda_3)+\mu_2(\lambda_3-\lambda_1)+\mu_3(\lambda_1-\lambda_2) \tag{13}$$

Equation (11) is the typical Rieman–Hilbert problem. We can derive the solutions for the problem as follows:

$$\Phi_k(Z_k)=\frac{(A_{k1}P+A_{k2}Q+A_{k3}D_2)}{2\pi(s-Z_k)}\left(\frac{a^2-s^2}{Z_k^2-a^2}\right)^{1/2} \quad (k=1,2,3) \tag{14}$$

where s refers to the distance between the traction acting point and the origin.

3. Pseudo-traction–electric displacement (PTED) method

Consider a two-dimensional infinite transversely isotropic piezoelectric ceramic containing N arbitrarily located cracks perpendicular to the poling direction of the material. As shown in Fig.

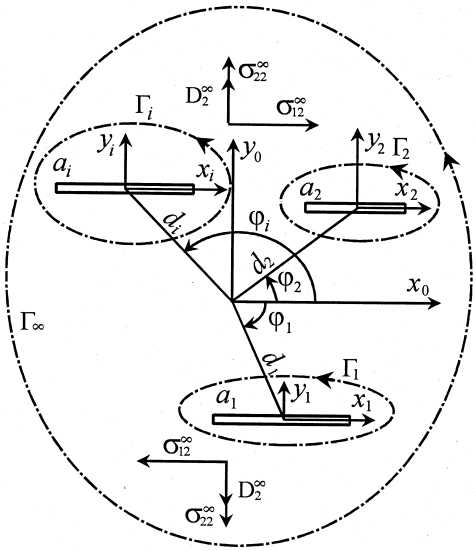

Fig. 2. The interaction problem among N cracks.

2, the loading conditions are the remote stresses σ_{22}^{∞} and σ_{12}^{∞} and the remote electric displacement D_2^{∞}. The local rectangular coordinate systems x_iy_i $(i = 1, 2, \ldots, N)$ are taken at the center of the ith crack, respectively. The direction of the y_i-axis is taken to be the poling direction of the material, while φ_i, d_i and a_i denote the location angle, location distance and the half-length of the ith crack.

All the crack faces are assumed to satisfy the traction-free conditions and the charge-free condition, i.e., $D_2 = 0$.

The interaction problem among N cracks shown in Fig. 2, can be decomposed into $N+1$ subproblems as treated by Horii and Nemat-Nasser (1985) in brittle solids.

In subproblem 1, the piezoelectric solid is loaded by remote stress σ_{22}^{∞} and σ_{12}^{∞} and the remote electric displacement D_2^{∞}. The normal stress $f_{ip0}(s)$, tangential stress $f_{iq0}(s)$ and the electric displacement $f_{iD0}(s)$ at any point $(s, 0)$ on the ith crack faces in the coordinate systems x_iy_i are:

$$\begin{aligned} f_{ip0}(s) &= \sigma_{22}^{\infty} \\ f_{iq0}(s) &= \sigma_{12}^{\infty} \quad i = 1, 2, \ldots, N \\ f_{iD0}(s) &= D_2^{\infty} \end{aligned} \tag{15}$$

In subproblem $i+1$ $(i = 1, 2, \ldots, N)$, the ith crack is subjected to the unknown pseudo-traction $P^i(x_i)$ and $Q^i(x_i)$ and the unknown pseudo-electric displacement $d_2^i(x_i)$. Of course, the total contributions of the pseudo-loading could be determined by using the well-known superimposing technique and by integrating the elementary solutions of the finite crack discussed in Section 2 along the crack length. After doing so, the normal stress $\sigma_{22}^{ji}(s)$, the tangential stress $\sigma_{12}^{ji}(s)$ and the second electric displacement component $D_2^{ji}(s)$ at any point $(s, 0)$ on the jth $(j \neq i)$ crack faces are then obtained as follows:

$$\sigma_{22}^{ji}(s) = \int_{-a_i}^{a_i} [f_{jpip}(x,s)P^i(x) + f_{jpiq}(x,s)Q^i(x) + f_{jpid}(x,s)d_2^i(x)]\,\mathrm{d}x$$

$$\sigma_{12}^{ji}(s) = \int_{-a_i}^{a_i} [f_{jqip}(x,s)P^i(x) + f_{jqiq}(x,s)Q^i(x) + f_{jqid}(x,s)d_2^i(x)]\,\mathrm{d}x$$

$$D_2^{ji}(s) = \int_{-a_i}^{a_i} [f_{jDip}(x,s)P^i(x) + f_{jDiq}(x,s)Q^i(x) + f_{jDid}(x,s)d_2^i(x)]\,\mathrm{d}x \tag{16}$$

where the normal stress $f_{jpip}(x,s), f_{jpiq}(x,s), f_{jpid}(x,s)$, the tangential stress $f_{jqip}(x,s), f_{jqiq}(x,s), f_{jqid}(x,s)$ and the electric displacement $f_{jDip}(x,s), f_{jDiq}(x,s), f_{jDid}(x,s)$ at the point $(s,0)$ on the jth crack faces, are induced from unit forces P and Q and the unit electric displacement D_2 located at a point $(x,0)$ on the ith crack faces, respectively (see Appendix) and $Z_k = \mathrm{Re}(Z) + \mu_k \mathrm{Im}(Z)$, $Z = d_j\,\mathrm{e}^{i\varphi_j} - d_i\,\mathrm{e}^{i\varphi_i} + s$.

As well known, the original problem is the superposition of the $N+1$ subproblems mentioned above, while the traction-free conditions and the charge-free conditions on all the crack faces should be met, which leads to the following integral equations.

$$P^i(s) + \sum_{j=0}^{N} \sigma_{22}^{ij}(s) = -f_{ip0}(s) \quad (j \neq i)$$

$$Q^i(s) + \sum_{j=0}^{N} \sigma_{12}^{ij}(s) = -f_{iq0}(s) \quad (j \neq i)$$

$$d_2^i(s) + \sum_{j=0}^{N} D_2^{ij}(s) = -f_{iD0}(s) \quad (j \neq i)$$

$$(i = 1, 2, \ldots, N) \tag{17}$$

Equation (17) is a system of integral equations with kernel functions $P^i(s)$, $Q^i(s)$ and $d_2^i(s)$ $(i = 1, 2, \ldots, N)$. By using the Chebyshev numerical integration method, the system can be transformed into a system of linear equations that can be solved with no further mathematical problem. So, the pseudo-tractions and the pseudo-electric displacement, i.e., $P^i(s)$, $Q^i(s)$ and $d_2^i(s)$ $(i = 1, 2, \ldots, N)$ distributed along all the crack faces can be obtained numerically. The stress and electric intensity factors of ith crack tips can then be obtained as follows:

$$K_{\mathrm{I}}^{\mathrm{R}i} = -\int_{-a_i}^{a_i} P^i(s)(a_i+s)^{1/2}(a_i-s)^{-1/2}/\sqrt{\pi a_i}\,\mathrm{d}s$$

$$K_{\mathrm{I}}^{\mathrm{L}i} = -\int_{-a_i}^{a_i} P^i(s)(a_i-s)^{1/2}(a_i+s)^{-1/2}/\sqrt{\pi a_i}\,\mathrm{d}s$$

$$K_{\mathrm{II}}^{\mathrm{R}i} = -\int_{-a_i}^{a_i} Q^i(s)(a_i+s)^{1/2}(a_i-s)^{-1/2}/\sqrt{\pi a_i}\,\mathrm{d}s \quad (i = 1, 2, \ldots, N)$$

$$K_{\mathrm{II}}^{\mathrm{L}i} = -\int_{-a_i}^{a_i} Q^i(s)(a_i-s)^{1/2}(a_i+s)^{-1/2}/\sqrt{\pi a_i}\,\mathrm{d}s$$

$$K_{\mathrm{e}}^{\mathrm{R}i} = -\int_{-a_i}^{a_i} d_2^i(s)(a_i+s)^{1/2}(a_i-s)^{-1/2}/\sqrt{\pi a_i}\,\mathrm{d}s$$

$$K_{\mathrm{e}}^{\mathrm{L}i} = -\int_{-a_i}^{a_i} d_2^i(s)(a_i-s)^{1/2}(a_i+s)^{-1/2}/\sqrt{\pi a_i}\,\mathrm{d}s \tag{18}$$

In the two-dimensional problems of piezoelectric ceramics, the J-integral defined by Pak (1990) and Suo et al. (1992), which has the clear physical significance as the total potential energy release rate, is given as the following formulation:

$$J = \int_\Gamma \frac{1}{2}(\sigma_{ij}\varepsilon_{ij} - D_iE_i)\,\mathrm{d}y - n_i\sigma_{ip}\frac{\partial u_{\mathrm{p}}}{\partial x_1}\,\mathrm{d}s - n_iD_i\frac{\partial \varphi}{\partial x_1}\,\mathrm{d}s \tag{19}$$

where u_{p} and φ are displacement and electric potential, respectively. Γ is a close integral contour.

The J-integrals $J^{\mathrm{R}i}$ and $J^{\mathrm{L}i}$ for the right and left tips of the ith crack, respectively, are functions of stress intensity factors and electric intensity factor. Following the ideas presented by Suo et al. (1992), the $J^{\mathrm{R}i}$ and $J^{\mathrm{L}i}$ integrals can be expressed by the intensity factors as:

$$J^{\mathrm{R}i} = \tfrac{1}{4}[K^{\mathrm{R}i}]^T H[K^{\mathrm{R}i}] \tag{20}$$

$$J^{\mathrm{L}i} = \tfrac{1}{4}[K^{\mathrm{L}i}]^T H[K^{\mathrm{L}i}] \tag{21}$$

where

$$[K^{\mathrm{R}i}] = [K_{\mathrm{II}}^{\mathrm{R}i} \quad K_{\mathrm{I}}^{\mathrm{R}i} \quad K_{\mathrm{e}}^{\mathrm{R}i}]^T \tag{22}$$

$$[K^{\mathrm{L}i}] = [K_{\mathrm{II}}^{\mathrm{L}i} \quad K_{\mathrm{I}}^{\mathrm{L}i} \quad K_{\mathrm{e}}^{\mathrm{L}i}]^T \tag{23}$$

H is a 3×3 matrix related to the material constants as:

$$H = 2\,\mathrm{Re}(iAB^{-1}) \tag{24}$$

where

$$[A] = \begin{bmatrix} p_1 & p_2 & p_3 \\ q_1 & q_2 & q_3 \\ r_1 & r_2 & r_3 \end{bmatrix} \tag{25}$$

$$[B] = \begin{bmatrix} -\mu_1 & -\mu_2 & -\mu_3 \\ 1 & 1 & 1 \\ -\lambda_1 & -\lambda_2 & -\lambda_3 \end{bmatrix} \tag{26}$$

and

$$p_k = a_{11}\mu_k^2 + a_{12} - b_{21}\lambda_k$$

Table 1
The reduced material constants of the PZT-4 piezoelectric ceramic

a_{11} 8.205×10^{-12}	a_{12} -3.144×10^{-12}	a_{22} 7.495×10^{-12}	a_{33} 19.3×10^{-12} ($m^2\ N^{-1}$)
b_{21} -16.62×10^{-3}	b_{22} 23.96×10^{-3}	b_{13} 39.4×10^{-3}	($m^2\ C^{-1}$)
δ_{11} 7.66×10^{7}	δ_{22} 9.82×10^{7}	($V^2\ N^{-1}$)	

$$q_k = (a_{12}\mu_k^2 + a_{22} - b_{22}\lambda_k)/\mu_k \quad k = 1, 2, 3$$
$$r_k = -(b_{13} + \delta_{11}\lambda_k)\mu_k \tag{27}$$

The mechanical strain energy release rate defined by Pak and Sun (1995a, b) have two modes. Their definition formulations are given as:

$$G_{\mathrm{I}}^{\mathrm{M}} = \lim_{\delta\to 0}\frac{1}{2\delta}\int_0^{\delta}\sigma_{22}(x)\Delta u_2(\delta - x)\,\mathrm{d}x \quad \text{for the Mode I} \tag{28}$$

$$G_{\mathrm{II}}^{\mathrm{M}} = \lim_{\delta\to 0}\frac{1}{2\delta}\int_0^{\delta}\sigma_{12}(x)\Delta u_1(\delta - x)\,\mathrm{d}x \quad \text{for the Mode II} \tag{29}$$

For the sake of convenience, only the Mode I is considered in this paper. $G_{\mathrm{I}}^{\mathrm{M}}$ can be re-expressed by the stress intensity factors and the electric displacement intensity factor as:

$$G_{\mathrm{I}}^{\mathrm{M}} = \tfrac{1}{4}(H_{21}K_{\mathrm{I}}K_{\mathrm{II}} + H_{22}K_{\mathrm{I}}^2 + H_{23}K_{\mathrm{I}}K_{\mathrm{e}}) \tag{30}$$

4. Numerical examples

Two numerical examples are presented in this section to give a fundamental understanding for the role that the electric displacement loading plays in the interaction problem. The PZT-4 ceramic is chosen as the piezoelectric material under consideration with the reduced material constants listed in Table 1 (Sosa, 1992). All the numerical calculations are performed under plane strain conditions.

First, the interaction problem of two cracks with equal lengths is considered under three kinds of compound mechanical–electric loading conditions, i.e. (i) $\sigma_{22}^{\infty} \neq 0$, $\sigma_{12}^{\infty} = 0$, $D_2^{\infty} = 10^{-8}\sigma_{22}^{\infty}\ \mathrm{C\,N^{-1}}$, (ii) $\sigma_{22}^{\infty} \neq 0$, $\sigma_{12}^{\infty} = 0$, $D_2^{\infty} = -10^{-8}\sigma_{22}^{\infty}\ \mathrm{C\,N^{-1}}$, (iii) $\sigma_{22}^{\infty} \neq 0$, $\sigma_{12}^{\infty} = 0$, $D_2^{\infty} = 0$. The last one is under the purely mechanical loading conditions of Mode I, whose results are well known. As shown by Sosa (1992) and Pak (1992), the electric displacement loading has no influence on the SIF's in the single crack problems in piezoelectric ceramics. However, it is not the case in the present interaction problem, i.e., the SIF's are no longer independent of the electric

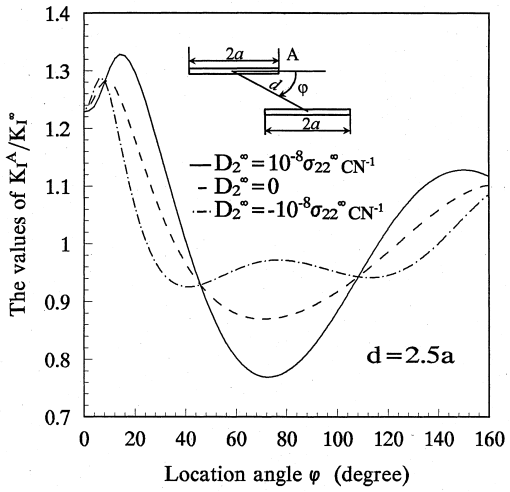

Fig. 3. The values of K_I^A/K_I^∞ change against location angle φ.

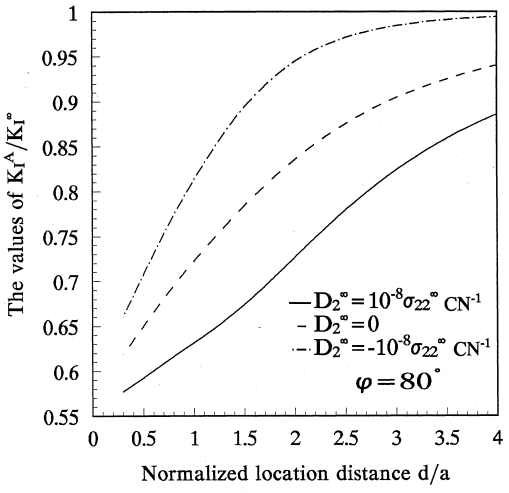

Fig. 4. The values of K_I^A/K_I^∞ change against normalized location distance d/a.

loading as they would be in the single crack problems (see Figs 3 and 4), since one of the cracks not only releases the stresses, but also disturbs the electric fields near the other crack induced by the electric displacement loading. The normalized SIF K_I^A/K_I^∞ at the tip A against the location angle φ is plotted in Fig. 3, while against the normalized distance d/a is plotted in Fig. 4. It is seen that the influence of the electric loading on the SIF at the tip A is significant. This conclusion could be given easily by making comparisons among the results derived under the three kinds of loading conditions mentioned above. The effect of the electric displacement loading on the SIF seems complicated. In the ranges of location angle φ between 8 and 46° and between 108 and 180°, the positive electric displacement loading has an effect increasing the SIF, while in the ranges between

Table 2
The values of fracture parameters change against d_n in the collinear case under the purely electric displacement loading conditions

$d_n=(d-a)/a$	0.1	0.2	0.5	1.0	1.5	2.0	3.0	4.0
K_e^A/K_e^∞	1.79	1.49	1.23	1.11	1.07	1.05	1.03	1.02
K_I^A/K_e^∞	0.00	0.00	0.00	0.00	0.00	0.00	0.00	0.00
K_{II}^A/K_e^∞	0.00	0.00	0.00	0.00	0.00	0.00	0.00	0.00

0 and 8° and between 46 and 108° it has an effect of decreasing the SIF. On the other hand, the negative electric displacement loading just has an opposite effect from those induced by the positive electric displacement loading (see Figs 3 and 4). This means that the effect of the electric loading on the SIF is governed not only by the electric loading level, but also by the relative locations of the interacting cracks. As could be imagined the SIF's are still independent of the electric displacement loading for the collinear case (see Table 2). Besides this, it is of interest to note that there are three special locations, i.e., $\varphi = 8$, 46 and 108°, at which the electric loading has no effect on the SIF K_I^A/K_I^∞. These special angles could be called the neutral electric displacement angles (NEDA). Moreover, it is seen that the positive electric loading increases the maximum amplification effect in the range of $K_I^A/K_I^\infty > 1$ and also increases the maximum shield effect in the range of $K_I^A/K_I^\infty < 1$. However, the negative electric loading has not the opposite tendency. As regards the MSERR which governs the crack growth in piezoelectric ceramics (Pak and Sun, 1995a, b), the electric displacement loading also has a significant effect on it. As shown in Fig. 5, the effect seems much stronger than that on the SIF discussed above. What is more, it is governed by the electric displacement loading level with no regard to the relative location angle φ. Here, G_I^{MA} is the MSERR

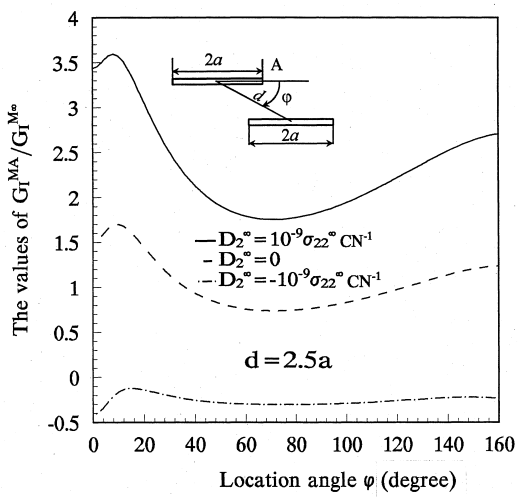

Fig. 5. The values of $G_I^{MA}/G_I^{M\infty}$ change against location angle φ.

Table 3
The values of normalized MSERR change against d_n in the collinear case under compound mechanical–electric loading conditions ($\sigma_{22}^{\infty} \neq 0, \sigma_{12}^{\infty} = 0, D_2^{\infty} = 10^{-9}\sigma_{22}^{\infty}$ C N^{-1})

$d_n = (d-a)/a$	0.1	0.2	0.5	1.0	1.5	2.0	3.0	4.0
$G_{\mathrm{I}}^{MA}/G_{\mathrm{I}}^{M\infty}$	7.33	5.06	3.44	2.82	2.60	2.50	2.40	2.35

at the tip A, while $G_{\mathrm{I}}^{M\infty}$ is the MSERR in a single crack problem with the same length under the purely mechanical loading conditions ($\sigma_{22}^{\infty} \neq 0$). The positive electric displacement loading makes the normalized MSERR $G_{\mathrm{I}}^{MA}/G_{\mathrm{I}}^{M\infty}$ increase. On the contrary, the negative electric displacement loading makes the MSERR decrease. In the collinear case, the MSERR is quite dissimilar to the SIF. Table 3 shows the results of $G_{\mathrm{I}}^{MA}/G_{\mathrm{I}}^{M\infty}$ in the collinear case. It is seen that, unlike the SIF, the MSERR is dependent on the electric displacement loading and that the dependence is still large although the normalized distance $d_n = (d-a)/a$ becomes very large.

Second, the interaction problem of two cracks with different lengths is considered. The results derived, respectively, under the compound mechanical–electric loading conditions and under the purely mechanical loading conditions are shown in Figs 6 and 7. The influence of the electric displacement loading on the SIF and the MSERR seems similar to that in the interaction problem of two cracks with equal lengths discussed above, although the neutral electric displacement angles for the case of $d_t = 0.15a$ (d_t is the distance between the tip A and the center of the short crack) became 15, 64 and 136°.

Finally, the difference between the TPERR and the MSERR is discussed for the interaction problem of two cracks with different lengths under the compound mechanical–electric loading conditions ($\sigma_{22}^{\infty} \neq 0, \sigma_{12}^{\infty} = 0, D_2^{\infty} \neq 0$). As shown in Fig. 8, the plotted curves against the electric

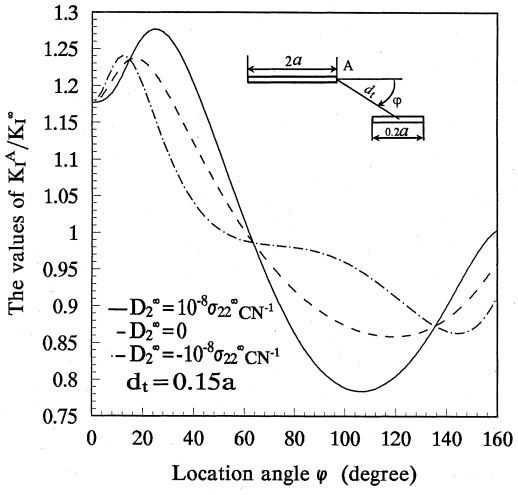

Fig. 6. The values of $K_{\mathrm{I}}^{A}/K_{\mathrm{I}}^{\infty}$ change against location angle φ.

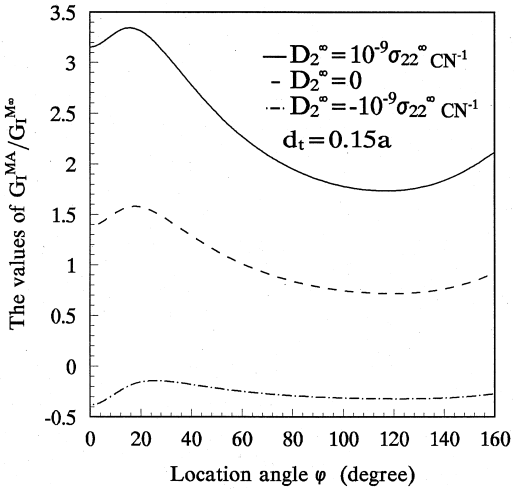

Fig. 7. The values of $G_{\mathrm{I}}^{MA}/G_{\mathrm{I}}^{M\infty}$ change against location angle φ.

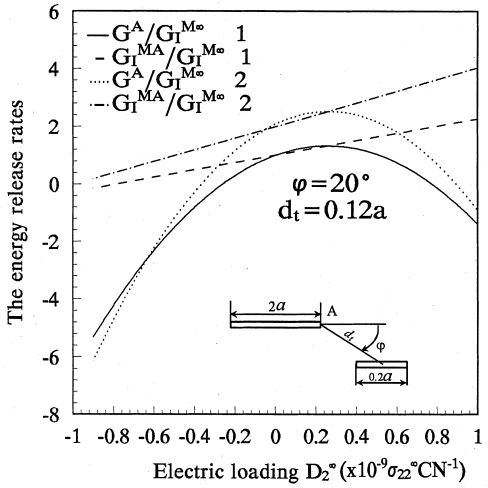

Fig. 8. The MSERR and the TPERR change against the electric displacement loading D_2^{∞}.

displacement loading D_2^{∞} with the legend 1 correspond to the single crack problem without interaction, while the curves with legend 2 correspond to the two cracks interaction problem. It is seen that the TPERR seems strongly dependent on the electric displacement loading level. Whatever, the electric loading is positive or negative, the TPERR always makes the negative values for larger electric loading levels. Quite contrary, the MSERR has a linear relation to the electric displacement loading level. As the electric loading increases from $D_2^{\infty} = -10^{-9}\sigma_{22}^{\infty}\ \mathrm{C\,N^{-1}}$ to $D_2^{\infty} = 10^{-9}\sigma_{22}^{\infty}\ \mathrm{C\,N^{-1}}$, the MSERR increases proportionally although the slope is different from that in the single crack problem.

Table 4
Numerical examinations by using a consistency check under compound mechanical–electric loading conditions ($\sigma_{22}^{\infty} \neq 0, \sigma_{12}^{\infty} = 0, D_2^{\infty} = 10^{-9}\sigma_{22}^{\infty}$ C N^{-1})

$\varphi = (d_t = 0.13a)$		30°	60°	90°	120°
Crack 1 ($2a$)	$K_{\mathrm{I}}^{\mathrm{R}}/K_{\mathrm{I}}^{\infty}$	1.2358	0.9918	0.8585	0.8110
	$K_{\mathrm{II}}^{\mathrm{R}}/K_{\mathrm{I}}^{\infty}$	−0.1141	−0.1809	−0.1183	−0.0152
	$K_{\mathrm{e}}^{\mathrm{R}}/K_{\mathrm{I}}^{\infty}$	1.1013	0.9796	0.9268	0.9054
	$K_{\mathrm{I}}^{\mathrm{L}}/K_{\mathrm{I}}^{\infty}$	1.0154	1.0137	1.0100	1.0058
	$K_{\mathrm{II}}^{\mathrm{L}}/K_{\mathrm{I}}^{\infty}$	0.0027	−0.0010	−0.0035	−0.0040
	$K_{\mathrm{e}}^{\mathrm{L}}/K_{\mathrm{I}}^{\infty}$	1.0103	1.0077	1.0054	1.0034
	$J^{(1)}$	−0.2940	−0.0993	0.0543	0.0909
Crack 2 ($0.2a$)	$K_{\mathrm{I}}^{\mathrm{R}}/K_{\mathrm{I}}^{\infty}$	0.7136	0.7496	0.7351	0.6573
	$K_{\mathrm{II}}^{\mathrm{R}}/K_{\mathrm{I}}^{\infty}$	0.0816	0.0212	−0.0895	−0.2049
	$K_{\mathrm{e}}^{\mathrm{R}}/K_{\mathrm{I}}^{\infty}$	0.6285	0.5962	0.5566	0.5047
	$K_{\mathrm{I}}^{\mathrm{L}}/K_{\mathrm{I}}^{\infty}$	1.0116	0.7098	0.4596	0.2491
	$K_{\mathrm{II}}^{\mathrm{L}}/K_{\mathrm{I}}^{\infty}$	−0.0569	−0.2296	−0.2741	−0.2379
	$K_{\mathrm{e}}^{\mathrm{L}}/K_{\mathrm{I}}^{\infty}$	0.7621	0.5431	0.3945	0.2696
	$J^{(2)}$	0.2940	0.0993	−0.0543	−0.0909
	J^{∞}	0.0000	0.0000	0.0000	0.0000

5. Consistency check

The numerical results are confirmed by using a consistency check proposed in this section. Turning back to see Fig. 2 and eqns (19)–(30), it is clear that the total contributions of multiple cracks to the J-integral (i.e., the TPERR) should be zero due to the remote loading conditions (Che and Hasebe, 1998):

$$J^{\infty} = J^{(1)} + J^{(2)} + \cdots + J^{(i)} + \cdots + J^{(N)} = 0 \tag{31}$$

where $J^{(i)}$ is evaluated along the Γ_i close contour in Fig. 2 and has the following relation with the J-integrals $J^{(\mathrm{R}i)}$ and $J^{(\mathrm{L}i)}$ of the right and left tips of the ith crack, respectively:

$$J^{(i)} = J^{(\mathrm{R}i)} - J^{(\mathrm{L}i)} \quad (i = 1, 2, \ldots, N) \tag{32}$$

When the SIF's and the EDIF of all the crack tips are known, the $J^{(i)}$ integral could be evaluated by using eqns (20) and (21) without any difficulties. Numerical examination for the two crack interaction problem with different lengths discussed above, different location angles, $\varphi = 30$, 60, 90 and 120°, and the same distance $d_t = 0.13a$ are shown in Table 4, in which the consistency check, i.e., eqn (31) is satisfied.

6. Conclusions and discussion

From the above performed discussions, the following conclusions are obtained:

(1) The PTED method is effective to treat multiple crack interaction problems in the piezoelectric

ceramics. This method is confirmed in this paper by using a consistence check specially proposed, i.e., eqn (31).

(2) The stress intensity factors at any tip for multiple crack interaction problems in piezoelectric ceramics are no longer independent of the electric displacement loading as they would be in the single crack problem. The dependence of the SIF's on the electric displacement loading is governed not only by the electric loading level, but also by the relative location of multiple cracks.

(3) There are the so-called NEDA at which the electric loading has no effect on the interacting SIF's. However, the angles are dependent on the normalized distance between the centers of multiple cracks.

(4) The electric displacement loading has much stronger effect on the mechanical strain energy release rate than on the Mode I SIF in the present interaction problem. The positive electric displacement loading makes the MSERR increase, while the negative electric displacement loading makes the MSERR decrease. Thus, the same conclusion could be given as Pak and Sun (1995a, b) did in single crack problems.

(5) The MSERR increases proportionally as the electric loading level increases from the negative values to positive values. This means that the positive electric loading aids the crack propagation while the negative electric loading impedes the crack propagation. The only difference of the MSERR curves between multiple crack problems and single crack problems is the slope along which the MSERR changes. In the present two parallel crack interaction problems, the slope of the MSERR is larger than that in single crack problems.

Acknowledgement

The authors wish to acknowledge that this work was supported by the Doctor Foundation of the Chinese National Education Commission.

Appendix

$$f_{jpip}(s) = G_1(\Phi_k(Z_k), Z_k) \quad (P = 1, q = 0, D_2 = 0)$$
$$f_{jqip}(s) = G_2(\Phi_k(Z_k), Z_k) \quad (P = 1, q = 0, D_2 = 0)$$
$$f_{jDip}(s) = G_3(\Phi_k(Z_k), Z_k) \quad (P = 1, q = 0, D_2 = 0)$$
$$f_{jpiq}(s) = G_1(\Phi_k(Z_k), Z_k) \quad (P = 0, q = 1, D_2 = 0)$$
$$f_{jqiq}(s) = G_2(\Phi_k(Z_k), Z_k) \quad (P = 0, q = 1, D_2 = 0)$$
$$f_{jDiq}(s) = G_3(\Phi_k(Z_k), Z_k) \quad (P = 0, q = 1, D_2 = 0)$$
$$f_{jpid}(s) = G_1(\Phi_k(Z_k), Z_k) \quad (P = 0, q = 0, D_2 = 1)$$
$$f_{jqid}(s) = G_2(\Phi_k(Z_k), Z_k) \quad (P = 0, q = 0, D_2 = 1)$$
$$f_{jDid}(s) = G_3(\Phi_k(Z_k), Z_k) \quad (P = 0, q = 0, D_2 = 1)$$

$$i = 1, 2, \ldots, N \quad j = 1, 2, \ldots, N \quad j \neq i$$

where $\Phi_k(Z_k)$ are the elementary solutions discussed in Section 2.

References

Chen, Y.H., Hasebe, N., 1998. A consistency check for strongly interacting multiple crack problems in isotropic, anisotropic and bimaterial solids. International Journal of Fracture, in press.

Horii, H., Nemat-Nasser, S., 1985. Elastic fields of interacting inhomogeneities. International Journal of Solids and Structures 21, 601–629.

Pak, S.B., Carman, G.P., 1997. Minimizing stress levels in piezoelectric media containing elliptical voids. ASME Journal of Applied Mechanics 64, 466–470.

Pak, S.B., Sun, C.T., 1995a. Fracture criteria for piezoelectric ceramics. Journal of the American Ceramic Society 78, 1475–1480.

Pak, S.B., Sun, C.T., 1995b. Effect of electric fields on fracture of piezoelectric ceramics. International Journal of Fracture 70, 203–216.

Pak, Y.E. 1990. Crack extension force in a piezoelectric material. ASME Journal of Applied Mechanics 57, 647–653.

Pak, Y.E. 1992. Linear electro-elastic fracture mechanics piezoelectric materials. International Journal of Fracture 54, 79–100.

Sosa, H., 1991. Plane problems in piezoelectric media with defects. International Journal of Solids and Structures 28, 491–505.

Sosa, H., 1992. On the fracture mechanics of piezoelectric solids. International Journal of Solids and Structures 29, 2613–2622.

Sosa, H., Pak, Y.E., 1990. Three-dimensional eigenfunction analysis of a crack in a piezoelectric material. International Journal of Solids and Structures 26, 1–15.

Suo, Z., Kuo, C.M., Barnett, D.M., Willis, J.R., 1992. Fracture mechanics for piezoelectric ceramics. Journal of the Mechanics and Physics of Solids 40, 739—765.